International Journal of Development and Sustainability
Online ISSN: 2168-8662 – www.isdsnet.com/ijds
Volume 2 Number 3 (2013): Pages 2093-2109
ISDS Article ID: IJDS13102501

Hydraulic characterization of the Kabatini Aquifer, Upper Lake Nakuru Basin, Kenya rift, using geophysical and pumping test data

Benjamin Sosi *

Department of Natural Resources, Egerton University, P.O Box 536, Egerton, Kenya

Abstract

The aim of the study was to characterize hydraulic parameters controlling groundwater occurrence in Kabatini aquifer of Lake Nakuru Basin, Kenya. The study utilized a combination of resistivity sounding and pumping test data. Vertical Electrical Soundings (VES) were carried out at close vicinity of eight drill sites, to relate geoelectric and hydraulic parameters. Resistivity data were analyzed using EarthImager 1D to obtain layer parameters within the constraints of lithology. This study has modified available petrophysical/pore-scale network relations and the bond shrinkage models so as to obtain a basis for applying geoelectrical methods in hydraulic parameter estimation. The adjustment has resulted into a calibrated field scale hypothetical comparison between transmissivity, T and apparent formation resistivity factor, Fa. A linear relationship ($\ln \mathrm{T} = -0.584 \ln \mathrm{F_a} + 2.054$; with correlation 82.9% percent), with a negative gradient between natural logarithm of transmissivity and apparent formation resistivity factor has been observed. The gradient of which is dependent on the bond shrinkage factor, x ($0 < x < 1$). An empirical accord between aquifer hydraulic parameters obtained from the resistivity and pumping test analysis emphasizes reliability of the methodology for groundwater flow assessment.

Keywords: Hydraulic parameter; Geoelectric parameter; Resistivity sounding; Pumping test; Kabatini

Cite this paper as: Sosi, B. (2013), "Hydraulic Characterization of the Kabatini Aquifer, Upper Lake Nakuru Basin, Kenya rift, Using Geophysical and Pumping Test Data", *International Journal of Development and Sustainability,* Vol. 2 No. 3, pp. 2093-2109.

* Corresponding author. *E-mail address:* sosibenja@gmail.com

1. Introduction

Knowledge of hydraulic parameters such as hydraulic conductivity/permeability (K), and Transmissivity (T), is vital for the determination of groundwater flow through earth materials. By extension, these aquifer characteristics are generally functional hydraulic parameters in groundwater flow modelling (Freeze and Cherry, 1979; Fitts, 2002). Singh (2005) suggests that the utilization of field hydrogeological evaluation techniques of is a normal approach for assessing these aquifer formation properties.

Geophysical methods can now contribute significantly towards their derivation and can greatly reduce the number of necessary pumping tests, which are both, time consuming and costly. Surface geophysical techniques have been found to be effective and fast for groundwater exploration and aquifer evaluation in this framework (Alridha et.al. 2013). Hubbard and Rubin (2002) in Singh (2005) approve the fact that geophysical methods generally are very effective for formation water saturation estimation, water quality assessment and depth to water table and bedrock determination. Although various geophysical techniques such as profiling, and also electrical tomography techniques currently are being applied to explore and assess water resources, the Schlumberger array vertical electrical sounding (VES) method still proves the most preferred since according to Jupp and Vozoff (1975) and Koefoed (1979) in Singh (2005) there exist standard, published direct and indirect interpretation techniques. In recent times, various research works (e.g. Brace, 1977; Biella et al., 1983; Singh, 2005; and, Odondi, 2009) have shown that integrated approach combining both geophysical and hydrogeologic methods can be used to obtain such hydraulic parameter estimates.

The present study utilized the integrated approach to parameterize the Kabatini aquifer. These constraints so established may provide optimal knowledge of the potentially porous media, because they link electric current transmission and groundwater flow, in the provisos of resistivity, permeability and layer thickness.

1.1. The Study Area

The study area is located within the plain area of Upper Lake Nakuru basin located in the eastern arm of the African Rift Valley (ARV) about 160 kms northwest of Nairobi. It is at the periphery of the country's fourth largest city whose populations depend on groundwater sources due to unreliable portable fresh surface water.

Geologically, the area is dominated by fractured volcanic rocks (lavas and pyroclastics) of Tertiary-Quartenary age, which are mantled by recent sediments. The fracturing of volcanic rocks can be attributed to the late subsidiary faults associated with Rift formation. Analyses of borehole lithology adjacent to station 1E,0 (Table 1) show thickness variation of the groundwater zone up to about 61 meters, with aquifer materials consisting commonly of volcano-clastic sediments, weathered/fissured trachytes, pumice and tuffaceous ash materials (Sosi, 2010).

Groundwater development in the Kabatini well field is such that borehole separation is generally below the established range of drilling. Boreholes even as close as fifteen meters are found (Figure 2). All wells are pumping twenty four hours a day. The cone of depression of such boreholes is dropped at a rate much rapid than if wells were to be drilled at a separation of at least four hundred meters apart.

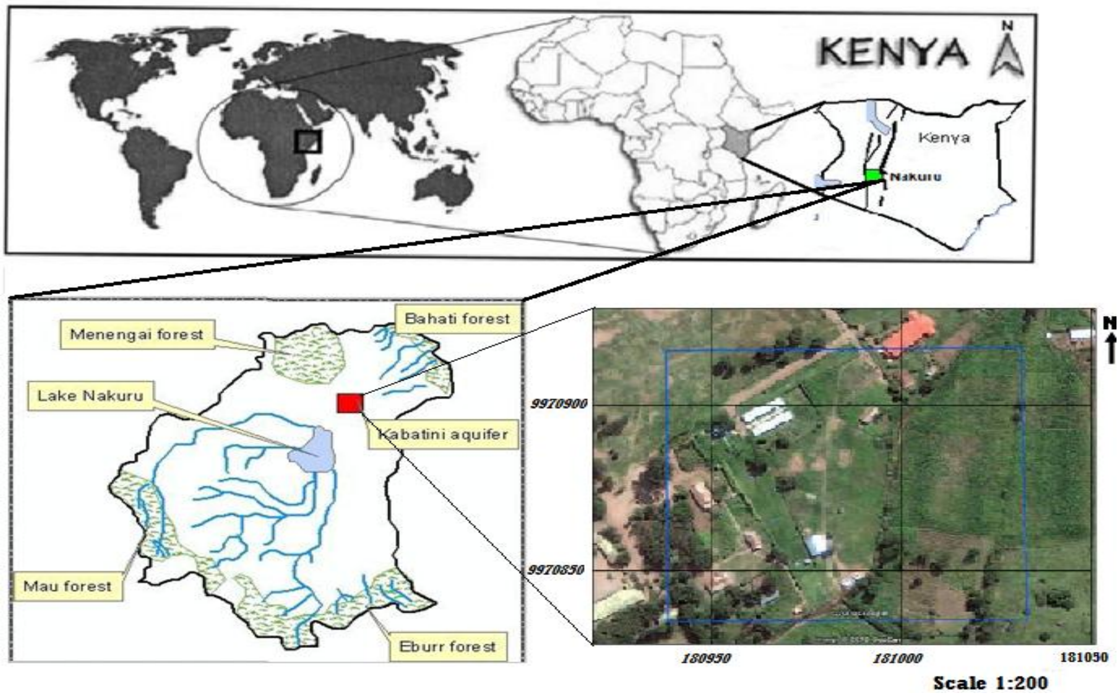

Figure 1. Location map of the study area. The blue border- line marks the extreme boundaries of the Kabatini well field.

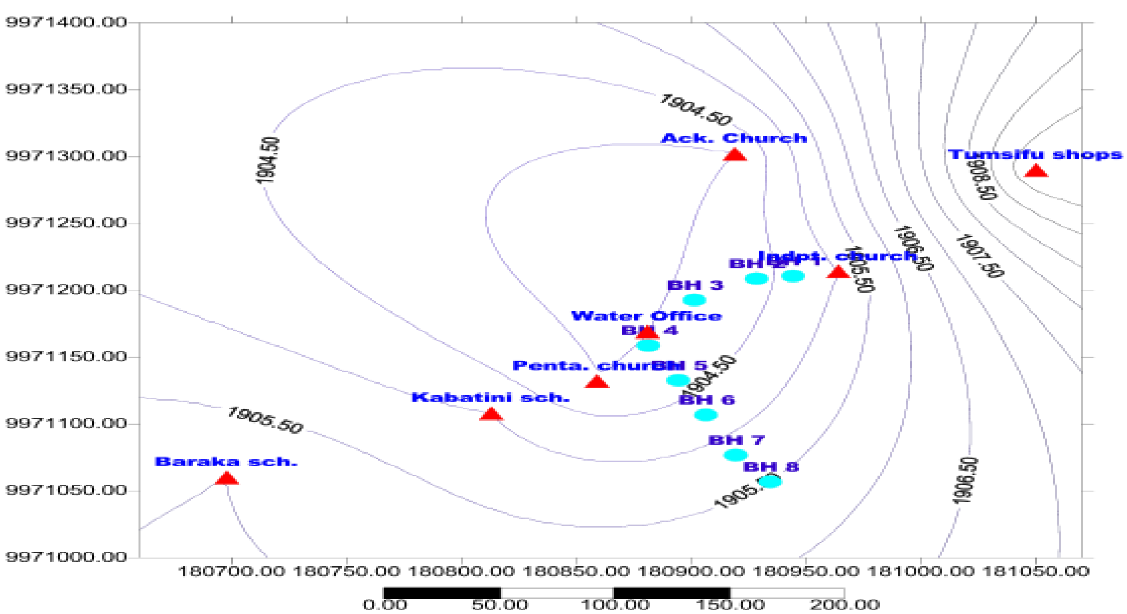

Figure 2. Location of Kabatini boreholes (closely separated circled light green marks labeled BH1, BH2, BH3… BH8)

2. Field data analysis and discussion of results

2.1. Resistivity data analysis

Geo-electrical data inversion was carried out for the spatially distributed hydraulic characteristics at the scale of field mapping using EarthImager 1D. Geoelectric resistivity models for each field stations were generated (Figure 3). The interpretation was however, based on the correlation between geologic logs from the well field and the modeled geoelectric profiles.

In fractured and fissured hard rock environment of the study area, delineation of aquifer characteristics by geophysical methods alone would be a very difficult task. Moreover, it is pointed out in Singh (2003a) that groundwater flow in fractured and/or fissured aquifers may be complicated, and accuracy in estimation of the hydraulic parameters depends on the hydraulic behaviour in particular fractures, which is site specific. Nevertheless, still it is a common routine during the step by step inversion process, to lump together thin undetectable layers so as to form one broad geoelectric layer. Doing so away from lithological logs sites (VES site 1E,0) and without enough independent constraints (on lithology and structure) is fraught with errors. This view is echoed in Telford et al (1990) who noted that uniqueness in resolving resistivity and thickness of a single layer cannot be achieved separately without adequate borehole data.

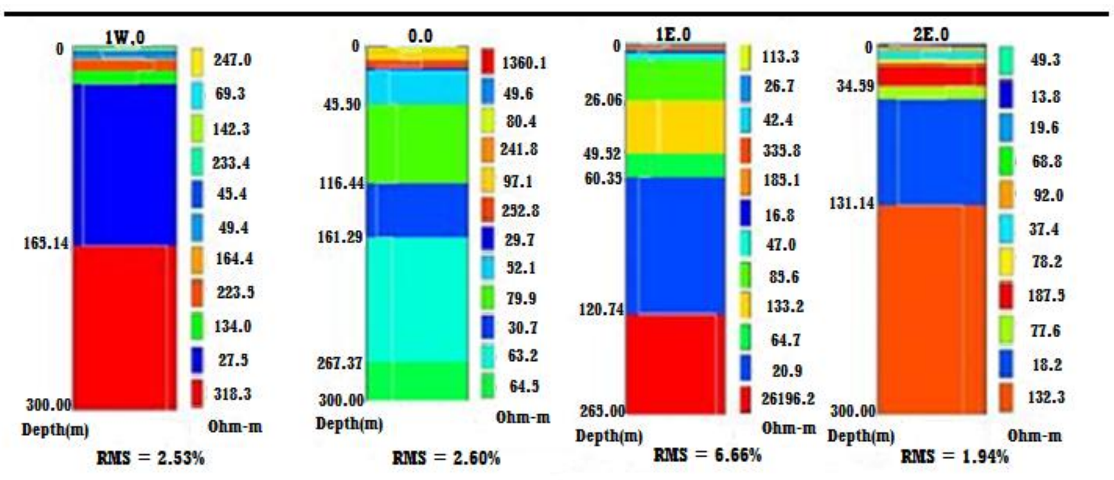

Figure 3. Geoelectric resistivity profile along west-east sounding traverses for W-E line. Field stations are shown at the top of each resistivity model.

Generally notable at all field stations is that two fundamental parameters namely resistivity and thickness can be used to describe each subsurface layer. There are the types HK at all sounding stations except stations 1W0,1E0, 2E1S and 1E2S where AHK type curves are exhibited. Most of the curves are HK type curves representing a model composed of a minimum of five geoelectric stratigraphic layers defined by layer resistivity relationship $\rho_1 > \rho_2 < \rho_3 > \rho_4 < \rho_5$ from the surface downwards. Based on geologic logs (Table 1) and geoelectric model (figure 3) visualization the model is at least composed of top volcanic soils (laterites and pyroclastic deposits), weathered trachytes, clay sandy sediments (unsaturated), tufficeous river sediments (aquifereous), and the impermeable basement rock. Although this basement rock is not seen in sounding stations predominantly to the south west where resistivity values < 20 Ohm- meters was observed.

Table 1. Borehole log compared with the vertical electrical sounding (VES) logs adjacent to VES station 1E,0. A borehole recently drilled next to the sounding point i.e station 1E0 struck water at a depth of 58 m

Borehole log		**VES log**	
Depth	**Rock Type**	**Depth**	**Resistivity (ohm-m)**
0 - 26	Loose volcani-clastic sediments mixed with argillaceous material ranging to brownish tuff and trachy- phonolite rocks at the bottom.	0 -1.4 1.4 – 2.4 2.4 – 26.0	High - Low resistivity High resistivity Low to moderate resistivity
26 - 62	Weathered erosional horizon intercalated between tuff and ash with few hard rock fragments and white patches of feldspar and ash at the top and basalt rock composed of a layer dominated by mafic minerals and subordinate quartz at the bottom.	26-62	Moderate to high resistivity
62 - 121	Loose volcanic sediments, weathered / fissured trachytes, pumice and pyroclastics	60-121	Low resistivity - 20.9 Ω (Groundwater horizon)
128 – 135	Greyish white tuff, not strongly indurated, and mixed with reddish mud varying to phonolitic trachyte	> 121	Very high resistivity

2.2. Pumping test data analysis

The pumping test data utilized in this study relates to particulars of four boreholes in the compound of the water office near Kabatini School. The boreholes are only thirty meters apart and are more or less in a straight line.

The geologic log (Table 1), resistivity log (Figure 3) water struck levels and water rest levels (Table 2) show that the aquiferous zone is confined. The upper confining layer being a thick layer of dark almost black basalt rock composed of a layer dominated by mafic minerals and subordinate quartz and the lower confining layer being a tough phonolitic trachyte.

Calculation of expected drawdown even if during a long time of pumping with no recharge of the aquifer (Kibunja, 1979) is shown in Table 4. The results have been used for respective drawdowns in all boreholes when each of them could pump at a time and others used as observation holes.

Table 2. Hydraulic particulars of Kabatini boreholes

Descri-ption	Depth (m)	W.S.L (m)	W.R. L (m)	D.W.L (m)	Yield (m3/hr)	Draw-down (m)	Spec. yield (m3/hr/m)
BH 4	147.7	68-72,94-96	26.92	31, 12	118.2	4.2	28.14
BH 5	166	49-52,93-122	28.16	33, 91	106.8	5.75	18.57
BH 6	150	52-54,102-108	27.73	31, 70	117.45	4.14	28.37
BH 7	150	43,98-100	25.44	35, 67	136.38	9.76	13.97

Source: (Kibunja, 1979)

Table 3. Elevations of the dynamic water levels (m) during test pumping

BH. No:	Groundwater level (m)	Drawdown (m)	Lowest observed static water level(m)	Elevation of dynamic water level (m)	Depth of drawdown in B.M (m)
4	1838.1	18.70	1805.56	1786.86	51.24
5	1837.5	19.04		1786.52	50.98
6	1837.8	19.04		1786.52	51.28
7	1837.1	18.70		1786.86	50.24

Source: (Kibunja, 1979)

Table 4. Drawdown in each borehole when one borehole is being pumped

	Observation borehole			
Pumped borehole	BH 4	BH 5	BH 6	BH 7
BH 4	5.84	4.47	4.26	4.12
BH 5	4.47	5.84	4.47	4.26
BH 6	4.26	4.47	5.84	4.47
BH 7	4.12	4.26	4.47	5.84
Total drawdown (m)	18.70	19.04	19.04	18.70

Source: (modified after Kibunja, 1979)

As borehole 4 and 7 were being tested in about the same time, the elevation of static water level was the same in other boreholes. According to Kibunja (1979), lowest elevation had been observed when borehole 5 was test pumped about 1.5 years earlier. The static water level was then 31.94 meters giving an elevation of the same at 1805.56 meters.

The discharge of borehole 7 was increased from 117.24 m3/hr to 136 (m3/hr) in the last two hours of the test. During test pumping of borehole 4, the levels in the other boreholes were also recorded (Table 4) and calculations of the aquifer hydraulic parameter were based on the records.

Based on static water levels shown in Table 2 and drawdowns in Table 4, hydraulic heads were computed in each borehole and presented in Table 5.

With each well used as pumping well at a time and the remaining wells as observation wells, a calculation is setup to obtain the hydraulic parameters one could expect. Use was made of the distance-drawdown formula of Theim for analysis of steady-state radial flows in Equation 1.

Table 5. Computed heads at both pumping test and observation sites.

Pumped borehole	Observation borehole			
	BH 4	BH 5	BH 6	BH 6
BH 4	1869.24	1869.37	1869.01	1871.44
BH 5	1870.61	1868.00	1868.80	1871.30
BH 6	1870.82	1869.37	1867.43	1871.09
BH 7	1870.96	1869.58	1868.80	1869.72

2.2.1. Calculation of hydraulic parameters

The water levels in the other boreholes were recorded only after pumping of one borehole for sufficiently long time. The boreholes are only 30 meters apart such that the furthest lies 90 meters from the pumped well. As the boreholes apparently lie in the same aquifer, this seems to be satisfactory. Based on the pumping test data an attempt is made to calculate the hydraulic characteristics of the aquifer using the Theim method of equilibrium pumping. This computation of hydraulic parameters has been achieved considering that steady-state radial flows towards each pumped well in the confined non-leaky aquifer after sufficiently long periods of pumping and that further drawdown observed in piezometers are essentially negligible.

The computed heads in observations boreholes in Table 5 and borehole separations were input in Equation 1 (after Theis, 1935);

$$T = \frac{Q}{\pi(h_2 - h_1)} ln\left(\frac{r_2}{r_1}\right) \qquad (1)$$

where, Q is the pumping rate T is the coefficient of aquifer transmissivity, h_1 is the head at distance r_1 and h_2 is the head at distance r_2 from the pumped well.

The data from these computation was used to predict the hydraulic characteristics of the aquifer (K and T)since the relation between drawdown and time is a function of aquifer permeability. A summary of the hydraulic and hydrogeological aquifer characteristics of some representative boreholes of the study area is represented in Table 6.

The specific capacity was computed by noting the drawdown in the pumped well after 24 hours of continuous pumping and multiplying it's reciprocal with the discharge rate of the specific well. Saturated vertical extent of the aquifer was interpreted from borehole completion records and also from geoelectric model layers of the adjacent VES stations. Aquifer hydraulic parameters (transmissivity, T, hydraulic and conductivity, K) have been computed mathematically using appropriate formulae for evaluating well characteristics from pumping test data.

Table 6. Summary of Pumping Test Results

[Borehole Number	4	5	6	7
Serial number (C prefix)	C4511	C4369	C4510	C4512
Pumping Rate (m^3/hr)	118.2	106.8	117.45	136.38
Drawdown after 24hr (m)	4.20	5.75	4.14	9.76
Specific capacity [(m^3/hr)/m]	28.14	18.57	28.37	13.97
Saturated thickness (m)	18.28	29.00	18.00	30.00
Transmissivity [(m^3/hr)/m]	9.968	17.072	8.932	11.003
Average field hydraulic conductivity [(m^3/hr)/m^2]	0.5453	0.5887	0.4962	0.3668

2.2.2. Geo-electrical and aquifer hydraulic parameter relationship

A critical account on the modification of Bernabe and Revil model so as to accommodate data for the Kabatini aquifer is given. It is this modification that allows relationship between Transmissivity as a hydraulic parameter and formation resistivity factor as a geo-electrical parameter to be developed. Dependence of hydraulic and electric flow gradient on the physical character (porosity) has been modeled using Archie‟s law (1942) (Equation 2):

$$\rho_f = F_a \rho_w \qquad (2)$$

where, the resistivity of the saturated rock, ρ_f is directly proportional to resistivity of the water filling the pores, ρ_w and F_a is the formation factor.

Since the conductivity of any medium is the reciprocal of its resistivity, the electrical component of the Bernabe and Revil (1995) model can alternatively be given in terms of bulk resistivity as;

$$\frac{1}{\rho} = \frac{1}{\rho_f}\frac{\sum_{\frac{cracks}{tubes}}^{n} V_p(n)\,|\nabla_\varphi(n)|^2}{V|\nabla_\varphi|^2} \qquad (3)$$

where, ρ is the bulk resistivity, and is the resistivity of water within the pores, Vp is the pore volume as envisaged in the three dimensional pore geometry of Bernabe and Revil, n is the number of pores through which flow occurs and V is the volume of heterogeneous material porous at pore scale. Electrical and hydraulic flow is modeled by establishing electrical gradient, ∇_φ and hydraulic gradient, ∇_φ across the network in the horizontal direction.

In the Wong et al (1984) modification, it is shown that the skewness in pore size distributions (implying power law relations between electrical and hydraulic parameters and pore volume and surface area) have strong dependence on rock forming minerals which tends to adjust pore sizes proportionally. In the bond shrinkage model, it is shown that as the steps get larger; a power law relationship develops from logarithmic ratios of mean Ø, wherein x; $0 < x > 1$ is the shrinkage factor by which the fracture elements are reduced, k is directly proportional to $\frac{\emptyset^{m_k}}{S^2}$ and m_k is defined;

$$m_k = \frac{2lnx^2}{x^2-1} + \frac{2}{x+1} > 0 \qquad (4)$$

The Wong et al (1984) relationship can be substituted into Bernabe and Revil electrical network equation 3. The resultant equation will be that $\frac{1}{\rho}$ is directly proportional to $\frac{1}{\rho_f}\emptyset^{(m_\emptyset)}$ wherein the exponent $m_\emptyset$ is expressed as;

$$m_\emptyset = \frac{lnx^2}{x^2-1} > 0;\ 0 < x < 1 \qquad (5)$$

The study also analyzed the dependance of field scale effects of the fracture medium (transmissivity, T and apparent formation resistivity factor, Fa) on pore structure impact on electrical and hydraulic flow in the saturated media. Transmissivity is related to hydraulic conductivity, K in Darcy's law. It is reflected in the site geometry of pore system and properties of the flowing fluid as a factor of its intrinsic permeability, k in Darcy's law. In terms of hydraulic conductivity (K), the transmissivity (T) of an individual fracture of an aperture (ac) can be expressed as;

$$T = a_c K = a_c k \frac{\delta g}{\mu} \tag{6}$$

The water flux therefore may be written as;

$$\mathrm{j}^{hydr} = \mathrm{q} = \frac{T}{a_c} \nabla h \tag{7}$$

Similarly electrical flow in the medium can be expressed in terms of current flux and potential gradient as;

$$\mathrm{j}^{hydr} = \frac{i}{A} = \frac{1}{\rho} \nabla V \tag{8}$$

The electrical property, the apparent formation resistivity factor (Fa) is expressed by Archie‟s law (Equation 2). In terms of apparent formation resistivity factor electric flow is therefore expressed as;

$$\mathrm{j}^{elect} = \frac{i}{A} = \frac{1}{F_a \rho_f} \nabla V \tag{9}$$

The apparent formation resistivity factor and aquifer transmissivity are respectively functions of porosity and pore connectivity. The use of the former in the study eliminates the effects of changes in saturation water resistivity but makes use of these changes. They have been respectively used to determine the aquifer‟s electrical and hydraulic particulars.

From the power laws of Wong et al (1984), proportionality relations between bulk resistivity and intrinsic permeability with porosity fraction on introducing proportionality constants, A and B respectively can be expressed as;

$$\frac{1}{\rho} = \mathrm{A} \frac{1}{\rho_f} \emptyset^{(\mathrm{m}_\emptyset)} \tag{10}$$

and;

$$\mathrm{k} = \mathrm{B} \frac{\emptyset^{(\mathrm{m}_k)}}{S^2} \tag{11}$$

To make k the subject, Equation 11 is divided by Equation 10 to obtain;

$$\mathrm{k} = \frac{B}{A} \emptyset^{(\mathrm{m}_k)} S^{-2} \rho_f \ \emptyset^{(-\mathrm{m}_\emptyset)} \ \rho^{-1} \tag{12}$$

Substituting for k in Equation 2, hydraulic conductivity, K can be expressed as;

$$K = \frac{\delta g}{\mu}\frac{B}{A}\emptyset^{(m_k)}S^{-2}\rho_f\ \emptyset^{(-m_\emptyset)}\ \rho^{-1} \qquad (13)$$

Equation 6 for calculation of transmissivity, T may be re-written as;

$$T = a_c\frac{\delta g}{\mu}\frac{B}{A}\emptyset^{(m_k)}S^{-2}\rho_f\ \emptyset^{(-m_\emptyset)}\ \rho^{-1} \qquad (14)$$

where $\emptyset = F_a{}^{\frac{-1}{m_\emptyset}}$ is Archie"s law (Archie, 1942); but from Equation 2, $\rho = F_a\rho_f$.

By replacing these values into Equation 14, we have;

$$T = a_c\frac{\delta g}{\mu}\frac{B}{A}\emptyset^{(m_k)}S^{-2}\rho_f\ \emptyset^{(-m_\emptyset)}\ F_a{}^{-1}\rho_f{}^{-1} \qquad (15)$$

Taking the natural logarithms of both sides of Equation 15, we obtain;

$$lnT = \ ln(\frac{Ba_c\delta g}{\mu A}S^{-2}) - \frac{m_k}{m_\emptyset}\ ln\ F_a{}^{-1}\rho_f{}^{-1} \qquad (16)$$

Equation 19 relates to parameters transmissivity, T and formation resistivity factor, Fa and is therefore the modified Bernabe and Revil relationship. The equation plots as a linear graph of the form $Y = a + bX$ where:

$$a = ln(\frac{Ba_c\delta g}{\mu A}S^{-2}) \text{ and } b = \frac{m_k}{m_\emptyset}$$

are coefficients between transmissivity and formation factor depicting the intercept and the slope respectively.

2.2.3. Calibration of the modified Bernabe and Revil model

The resistivities of collected water samples were determined on site to compute the formation factor (F_a) in Table 6 and porosity in Table 7. The fundamental principle of application of resistivity methods in hydrogeology is the utilization of the dependence of rocks resistivity on the lithology of them and mineralogy of water filling the pores. The resistivity of an aquifer is therefore related to Electrical Conductivity (EC) of its water.

In the fractured volcano-sedimentary setting of the study area, groundwater flow is mainly through fractures and apertures with minimum clay content which partially satisfies the requirements set out in Equation 2. It was a working hypothesis for this study that it is the number and distribution of fractures, and the effective porosity of each geological material that control aquifer characteristics. This observation was simulated by considering a confined heterogeneous porous medium, within which pores are composed of cracks and fractures of constant width in the flow direction.

Table 6. Hydraulic and geoelectric parameters at the pumping test sites.

Borehole number (C-prefix)	Transmissivity, T (m2/hr)	Measured pore-water resistivity, ρ_w (Ohm – m)	Observed aquifer Resistivity, ρ_f (Ohm–m)	Formation resistivity factor, Fa
4 (C4511)	9.968	18.18	34.33	0.53
5 (C4369)	17.072	18.18	65.28	0.28
6 (C4510)	8.932	18.18	25.33	0.72
7 (C4512)	11.003	18.18	25.45	0.71

The hydraulic data and geoelectric data are derived by correct substitution in Equation 6 and Equation 2 respectively. Figure 4 is a plot of values of natural logarithm of formation resistivity factor, Fa derived from geo-electrical resistivity sounding against values of natural logarithm of transmissivity, T computed from pumping test data.

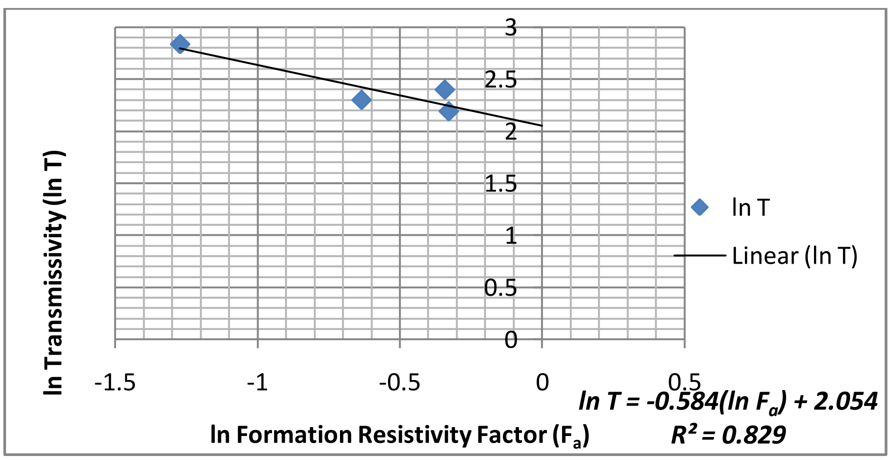

Figure 4. Calibrated modified Bernabe and Revil model for the study area.

The data plotted are those for logarithms of transmissivity values as the slope and intercept values are in whereas formation factor; being a ratio of resistivity values has no units. The resultant graph gives a negative gradient in conformity with hypothetical computations postulated by Equation 16, that is, electrical flow through pore volumes rather than through clay surfaces. The observed correlation is expressed by way of linear regression techniques by Equation 17.

$$\ln T = -0.584(ln\ Fa) + 2.054 \qquad (17)$$

Equation 17 is therefore the calibrated model approximated for the Kabatini aquifer. The model is less robust with regard to a correlation coefficient of only 82.9% (percent) showing that apparent resistivity factor is fairly well correlated with transmissivity. This is because transmissivity evaluations based on borehole records could be particularly erroneous if the saturated thicknesses are not recorded properly.

In order to harmonize the calibrated model of the Kabatini aquifer in Equation 17 and the modified Bernabe and Revil model (Equation 16), the slope is expressed in terms of bond shrinkage factor, x as;

$$b = \frac{m_k}{m_{\emptyset}} = \left[\frac{2lnx^2}{x^2-1} + \frac{2}{x+1}\right]\left[\frac{lnx^2}{x^2-1}\right] = 0.585 \qquad (18)$$

Equation 18 can be re-written as;

$$\frac{m_k}{m_{\emptyset}} = \left[2 + \frac{2(x-1)}{\ln x^2}\right] = 0.585 \qquad (19)$$

This equation further reduces to;

$$2x - 2 = \ln x \qquad (20)$$

Equation 20 can be split into two equations given by;

$$\mathrm{y} = 2x - 2 \qquad (21)$$

and,

$$\mathrm{y} = \ln x \qquad (22)$$

With approximations of x and y values, the two functions in Equations 21 and 22 were plotted on the same graph for values of $0 < x < 1$. The point of intersection of the two functions shown in figure 5 is the numeric solution required.

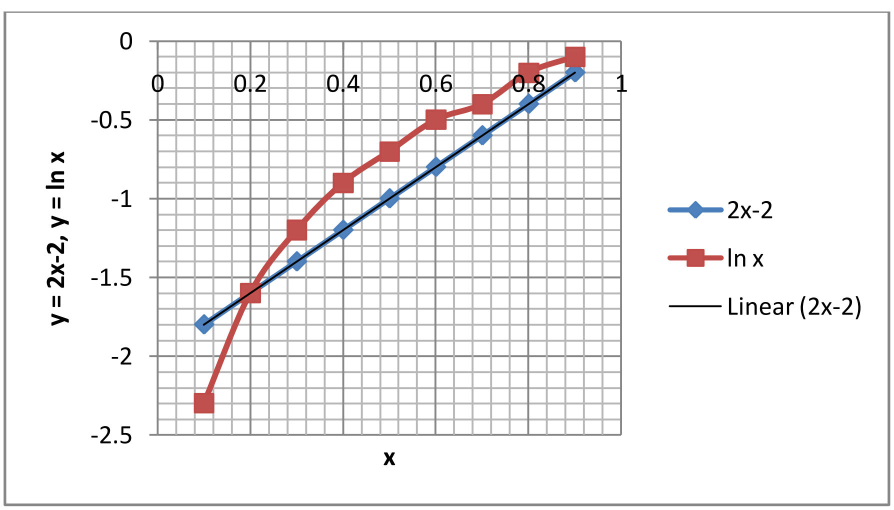

Figure 5. Estimated values of f(x) = y, y = 2x-1 and y = ln x for 0< 0 > 1. The intersection of the two curves gives a numeric solution to Equation 5.

Examination of the two curves reveals that the two curves intersect at x = 0.2 for values of $0 < x < 1$. Therefore the cementation factor exponent $m_{\emptyset}$ expressed by Equation 5 will be 4.02.

2.2.4. Geoelectric models of porosity, transmissivity and hydraulic conductivity

The cementation exponent so obtained was used in the computation of porosity values at each VES station given that conductivity of groundwater was observed to be 550μS/cm. Archie‟s law (1942) in Equation 2 enabled the estimation of porosity from geoelectrical sounding data. With the development of the geoelectric-hydraulic relationship in Equation 17, it was possible to compute transmissivity across the study area. Values for hydraulic conductivity, K were derived from transmissivity Equation 6 in which the pore scale fracture aperture (a_c) is replaced by the field scale aquifer thickness (b_e).

Table 7. Calculated porosity, transmissivity and hydraulic conductivity values for the study area

Station	Aquifer Resistivity (Ω-m)	Aquifer Thickness, b_e	Calculated Formation Factor, F_a	Calculated Porosity $\emptyset = \left[\frac{1}{F_a}\right]^{4.02}$	ln T = -0.584(ln F_a) + 2.054	Aquifer Transmissivity, T (m³/hr)	$K = \frac{T}{b_e}$ (m²/hr)
1W,0	2.94	16.41	6.18367	61.8848	0.9882	2.6863	0.1637
0,0	51.85	21.92	0.35063	56.0517	2.6671	14.3981	0.65685
1E,0	83.8	34	0.21695	55.9181	2.948	19.0667	0.56079
2E,0	26.75	9.89	0.67963	56.3807	2.2799	9.776	0.98847
1W,1S	20.53	45.39	0.88553	56.5866	2.1251	8.3739	0.18449
0,1S	34.33	40.15	0.52957	56.2307	2.4259	11.3122	0.28175
1E,1S	18.04	70.57	1.00776	56.7089	2.0495	7.7638	0.11002
2E,1S	55.03	-	0.33037	56.0315	2.7019	7.9401	-
1W,2S	15.4	-	1.18052	56.8816	1.9569	7.0775	-
0,2S	96.24	-	0.1889	55.89	3.0289	20.6748	-
1E,2S	8.46	36.27	2.14894	57.85	1.6065	4.9853	0.13745
2E,2S	20.9	36.81	0.86986	56.571	2.1356	8.4618	0.22988
1W,3S	14.12	86.2	1.28754	56.9886	1.9062	6.7272	0.07804
0,3S	16.97	50.39	1.0713	56.7724	2.0137	7.491	0.14866
1E,3S	33.93	20	0.53581	56.2369	2.419	11.2349	0.56175
2E,3S	32.23	57.71	0.56407	56.2652	2.389	10.9021	0.18891

Nevertheless still, it was finally possible to refine our approximate transmissivity – formation factor model in Equation 17 graphically by plotting the values for natural logarithm of transmissivity against natural logarithm of formation factor given that now we have sufficient data in Table 7.

The resulting graph yields a highly correlated data with product moment correlation coefficient =1 (Figure 6). Comparison in terms of factor of R^2 is made between the model with that in Figure 4. It was noted that this plot is more sensitive in the provisos defined. The trend and nature of transmissivity-formation resistivity factor relationship for the study area was therefore established as:

$$ln\,T = -0.584(ln\,Fa) + 2.054.$$

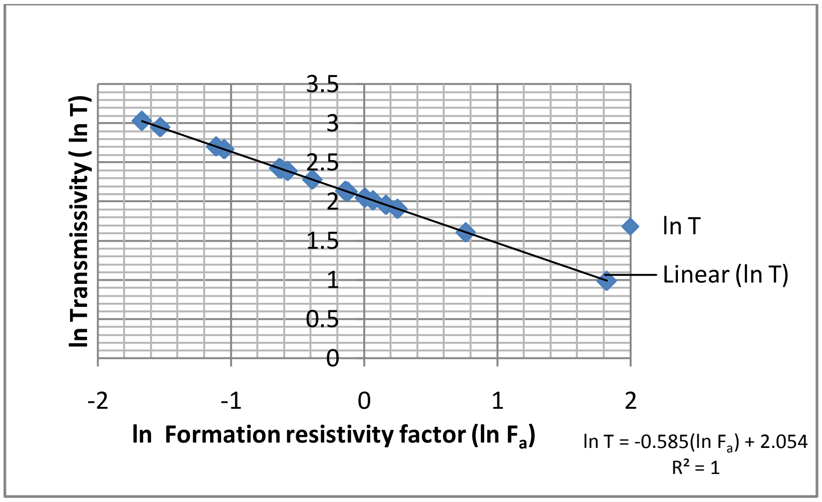

Figure 6. A more sensitive model showing natural logarithm of transmissivity – formation factor relationship

3. Conclusions

The application of the resistivity measurements and pumping test data permitted the extrapolation of pore-scale hydraulic parameters within the study area. Measurements of the ground water resistivity led to derivation of the approximate calibrated model for the Kabatini aquifer. Use of layer thickness, as derived from the interpretation of resistivity soundings data and transmissivity calculated on the basis of both pumping test and geophysical data led to the calculation of aquifer hydraulic conductivity.

This study has utilized the pore-scale network relations developed by Bernabe and Revil (1995) and the bond shrinkage model by Wong et al (1984). A calibrated linear relationship with a negative correlation between natural logarithm of transmissivity, T and apparent formation resistivity factor, F_a in Equation 17 has been observed. The gradient of this linear relation is dependent on the bond shrinkage factor, x (0 < x < 1) of Wong et al (1984). It determines sizes of the pore volumes in the flow medium. The negative correlation coefficient implies that flow through pore volume increases proportionally with transmissivity but inversely with apparent formation resistivity factor.

Acknowledgement

The presented work was carried out as part of the Master of Science (Geology) Degree program. The realization of this project was funded by the University of Nairobi, Kenya. The author is also sincerely thankful to Prof. Justus O. Barongo, for providing some field equipments.

References

Alridha, N.A., Ameen, I.A. and Wadhah, M.S.K. (2013), "The Role of (Geoelectric and Hydrogeologic) Parameters in the Evaluation of Groundwater reservoir at South of Jabal Sinjar area", *Iraqi Journal of Science,* Vol. 54, No. 3, pp. 628-637.

Archie, G.E. (1942), "The electrical resistivity log as an aid in determining some reservoir characteristics", *Trans. Am. Inst. Min. Metal. and Petr. Eng.,* Vol.146, pp. 54-62.

Bernabe, Y. and Revil, A. (1995), "Pore scale heterogeneity, energy dissipation and the transport properties of rocks", *Geophys Res. Lett.* Vol. 22, No. 12, pp. 1529-1532.

Biella, G., Lojez, A. and Tabacco, I. (1983), "Experimental study of some of hydrogeophysical properties of unconsolidated media", *Groundwater Journal,* Vol. 21, pp. 741–751.

Brace, W.F. (1977), "Permeability from resistivity and pore shape", *Journal of Geophys. Res.,* Vol. 82, No.23, pp. 334–339.

Fitts, C.R. (2002), *Groundwater Science,* Elsever Publications, the Netherlands, p. 167- 175.

Freeze R.A. and Cherry, J.A. (1979), *Groundwater,* Prentice Hall Inc. Englewood Cliffs, New Jersey.

Hubbard, S. and Rubin, Y. (2002), "Hydrogeophysics: State-of-the-Discipline", *EOS,* Vol. 83, No. 51, pp. 602-606.

Jupp, D.L.V. and Vozoff, K. (1975), "Stable iteration method for inversion of geophysical data", *Journal of Geophys. Roy. Astr. Soc.* Vol. 42, pp. 957–976.

Kibunja, S.K. (1979), "*Augmentation Kabatini boreholes, Design report". Working Paper No.125.* Nakuru Municipal Water Supply. Ministry of water development, Nairobi, 50 pp.

Koefoed, O. (1979), *Geosounding Principle-1, Resistivity sounding measurements,* Elsevier Science Publications, New York.

Odondi, M.K. (2009), "Integrated approach utilizing geoelectric resistivity data to groundwater modelling in the hard rock terrains of the Jangaon watershed of India." A PhD thesis. Jomo Kenyatta University of Agriculture and Technology, Kenya. 193 pp.

Singh, K.P. (2003a), "A New Approach for Detection of Hidden Aquifer Using DC Resistivity Data Transforms", *Journal of Geol. Soc. India,* Vol. 61, pp. 540–548.

Singh, K.P. (2005), “Nonlinear estimation of aquifer parameters from surficial resistivity measurements”, *Journal of Hydrol. Earth Sys. Sci. Discuss.,* Vol. 2, pp. 917–938.

Telford, W., Geldart, L. and Sherrif, R. (1990), *Applied Geophysics,* Cambridge University Press, U.K.

Sosi, B. (2010), “Hydraulic Characterization of the Kabatini Aquifer, Upper Lake Nakuru Basin, Kenya rift, Using Geophysical and Pumping Test Data”, available at: http://geology.uonbi.ac.ke/node/935 (accessed on 10 March 2011).

Theis, C.V. (1935), “The relation between the lowering of the piezometric surface and the rate and duration of discharge of a well using groundwater storage”, *Am. Geophysics Union, Trans.,*Vol. 16, pp. 501-524.

Wong, P., Koplick, J. and Tomanic, J.P. (1984), “Conductivity and Permeability of Rocks”, *Phys. Rev, B.,* Vol. 30, pp. 6606-6614.